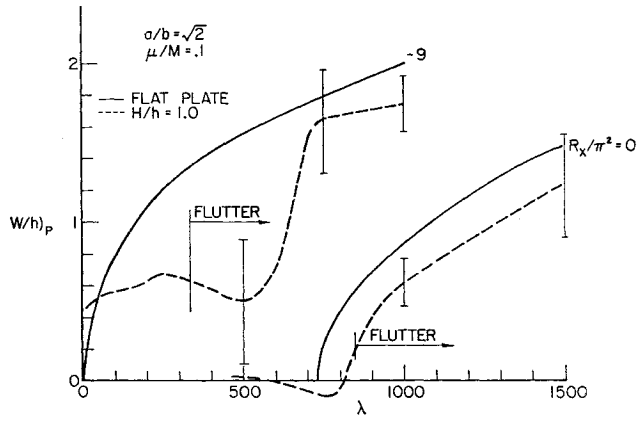

Fig. 3 Plate deflection vs dynamic pressure.

the flutter oscillation of an imperfect plate is no longer symmetrical about its shape. As may be seen the change from the flat plate result is very modest for no in-plane load $R_x/\pi^2 \equiv 0$; however, for $R_x/\pi^2 = -9$ the change is very substantial. Hence in Fig. 4 we plot the dynamic pressure at the onset of flutter, λ_f vs maximum rise height for $R_x/\pi^2 = -9$. Note the significant effect even for imperfections small compared to the plate thickness. Finally in Fig. 5 we plot λ_f vs R_x for a flat plate and an imperfect plate.

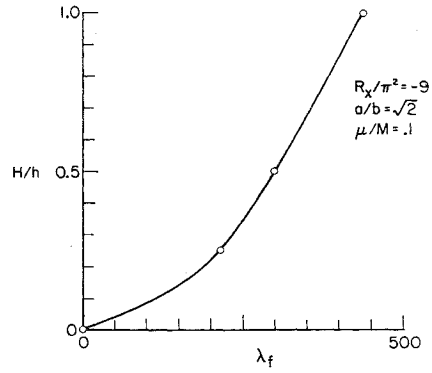

Fig. 4 Rise height vs flutter dynamic pressure.

From these results we make a second important observation. For an imperfect plate flutter will never begin at $\lambda \equiv 0$. However for nearly perfect plates it should be possible to approach this result.

Conclusions

Based upon the present results, and quite aside from any possible effect of structural damping, it is seen that any realistic, i.e., imperfect, plate will not flutter at zero dynamic pressure. The flutter dynamic pressure will depend upon the magnitude (and distribution) of the initial imperfections. Further the present results suggest the difficulty of experimentally establishing the flutter boundary under conditions at very low dynamic pressure. While the plate will flutter, the amplitude may be sufficiently small so that it is indistinguishable from plate response to flow noise. Finally, even for a perfect plate in the absence of flow noise, an aeroelastic instability only occurs under trivial conditions at zero dynamic pressure, i.e., zero plate amplitude.

The implications for design are obvious. A rational design may be based on either 1) maximum permissible plate deflection or stress or 2) the inclusion of realistic plate imperfections.

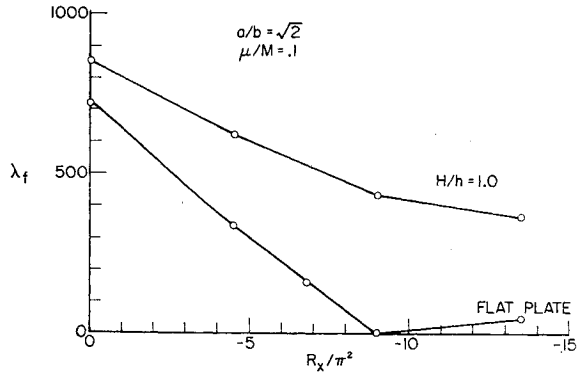

Fig. 5 Flutter dynamic pressure vs in-plane load.

References

[1] Shore, C. P., "Flutter Design Charts for Stressed Isotropic Panels," *AIAA Structural Dynamics and Aeroelasticity Specialist Conference*, AIAA, New York, 1969.

[2] Erickson, L. L., "Supersonic Flutter of Flat Rectangular Orthotropic Panels Elastically Restrained Against Edge Rotation," TN D-3500, 1966, NASA.

[3] Shideler, J. L., Dixon, S. C., and Shore, C. P., "Flutter at Mach 3 of Thermally Stressed Panels and Comparison with Theory for Panels with Edge Rotational Restraint," TN D-3498, 1966, NASA.

[4] Shore, C. P., "Effects of Structural Damping on Flutter of Stressed Panels," TN D-4900, 1968, NASA.

[5] Dowell, E. H. and Ventres, C. S., "Nonlinear Flutter of Loaded Plates," AIAA Paper 68-286, Palm Springs, Calif., 1968.

[6] Ventres, C. S. and Dowell, E. H., "Influence of In-Plane Edge Support Flexibility on the Nonlinear Flutter of Loaded Plates," *AIAA Structural Dynamics and Aeroelasticity Specialist Conference*, AIAA, New York, 1969.

[7] Dowell, E. H., "Nonlinear Flutter of Curved Plates," *AIAA Journal*, Vol. 7, No. 3, March 1969, pp. 424–431.

Stagnation Temperature and Molecular Weight Effects in Jet Interaction

R. A. Chambers* and D. J. Collins†
Naval Postgraduate School, Monterey, Calif.

In a recent paper by Chrans and Collins,[1] the effects of injectant stagnation temperature and injectant molecular weight variations on the flowfield generated by secondary injection were determined experimentally. The purpose of this Note is to extend their work to consider the effect of these two variables on the interaction side force and the amplification factor. Relationships between the side force and penetration height (h) and between side force and the characteristic radius (R_o) of the blast wave theory are also developed.

Experiments were conducted in the Naval Postgraduate School supersonic wind tunnel at a primary Mach number of 1.92. The interaction side force was determined from the integration of the pressure measured from 47 pressure ports in the base of the wind tunnel. The geometric pattern of the pressure ports and the associated recording system are discussed in Refs. 2 and 3. The ratio of injectant stagnation pressure to freestream stagnation pressure ($P_{oj}/P_{o\infty}$) ranged from $\frac{2}{3}$ to 6, whereas the ratio of injectant stagnation tem-

Received October 3, 1969; revision received November 24, 1969. This was supported by Naval Air Systems Command Contract A33-330/551/69.

* Captain, U.S. Marine Corps.

† Professor of Aeronautics. Associate Fellow AIAA.

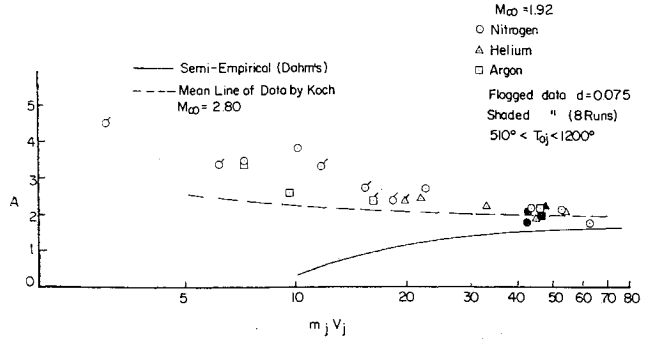

Fig. 1 Force amplification factor vs secondary momentum flux.

perature to freestream stagnation temperature ($T_{oj}/T_{o\infty}$) ranged from 1 to 2.4.

Injection was normal to the tunnel wall from a sonic circular port. Two different injection diameters (0.1406 in. and 0.075 in.) were used. Argon, helium and nitrogen were used as test gases. This gave a fairly wide variation in molecular weight.

Figure 1 shows a plot of the amplification factor

$$A = (F_i + F_j)/F_j$$

plotted vs the secondary momentum. F_i is the interaction side force and F_j is the force of the jet. The data correlates well as a function of the secondary momentum. No systematic variation with molecular weight or heating can be seen. At the higher values of momentum flux reasonable agreement with values predicted by Dahm's semiempirical second-order theory[4] is obtained. A mean line of the injection data obtained by Koch[2] at a Mach number of 2.80 is also shown on the figure. This data was obtained using a flat plate with the identical pressure port distribution as that used for the $M = 1.92$ data. At the higher secondary momentum or higher injection stagnation pressure no influence of Mach number is observed.

In accordance with the theoretical development of Dahm[4] the side force is

$$F_i \propto R_0^{3/2}$$

while in the theory of Zukoski and Spaid[5] one has

$$F_i \propto h^2$$

Figure 2 shows the side force plotted in turn as a function of the two characteristic dimensions (R_o,h). Less scatter is observed in the plot of F_i vs R_o since R_o is a calculated quantity. Although the data at higher values of R_o agrees somewhat with $R_o^{3/2}$, the over-all trend of the data is more closely represented by R_o to the first power. In the plot of F_i vs h the trend of the data is also more closely represented by h

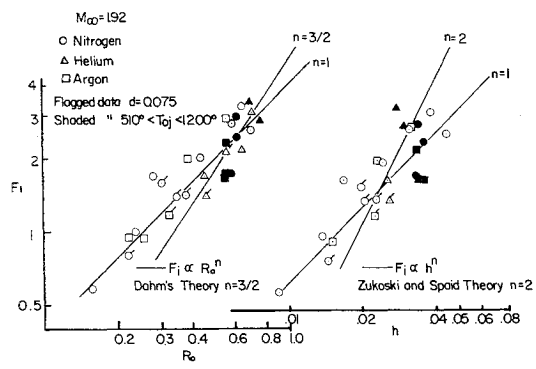

Fig. 2 Interaction side force vs blast wave characteristic radius, and penetration height.

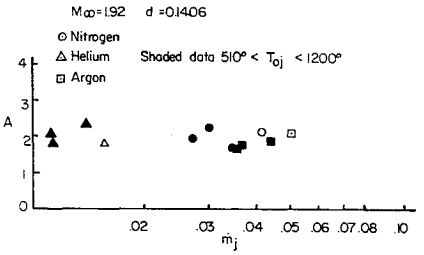

Fig. 3 Force amplification factor vs secondary mass flow rate (P_{oj} = 120).

rather than h^2. Within the range of the data one can conclude, as was the case in Ref. 1, that h and R_o are equivalent characteristic dimensions for jet interaction.

The final series of tests were directed at the question of the dependence of the amplification factor on secondary mass flow and secondary stagnation temperature variations.

In Fig. 3, the amplification factor is plotted as a function of secondary mass flow rate ($\dot{m}_j$) for constant P_{oj} = 120 psia. The graph includes data from all three test gases as well as secondary stagnation temperature variations. In Fig. 4, the same data is plotted as a function of secondary stagnation temperature. Within the scatter of the data the amplification factor, for constant P_{oj}, is independent of the mass flow and the stagnation temperature.

The results of this article extend the work of Chrans and Collins to include the case of side force and amplification factor. A connection is made between side force and penetration height, and between side force and the characteristic radius of blast wave theory. The momentum of the injectant is the determining variable both for the geometry of the flowfield and the side force generated by the interacting jet.

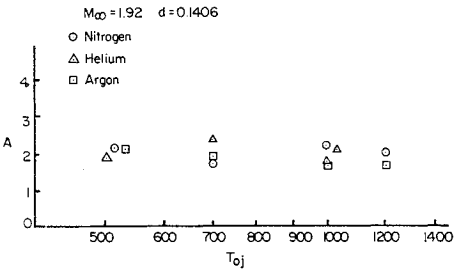

Fig. 4 Force amplification factor vs secondary total temperature (P_{oj} = 120).

References

[1] Chrans, L. J. and Collins, D. J., "The Effect of Stagnation Temperature and Molecular Weight Variation on Gaseous Injection into a Supersonic Stream," *AIAA Journal*, Vol. 8, No. 2, Feb. 1970, pp. 287–293.

[2] Koch, L. N., "The Effect of Varying Secondary Mach Number and Injection Angle on Secondary Gaseous Injection into a Supersonic Flow," Aeronautical Engineer thesis, June 1969, U.S. Naval Postgraduate School, Monterey, Calif.

[3] Chambers, R. A., "The Effect of Varying Secondary Stagnation Temperature and Molecular Weight on the Side Force Generated by Gaseous Injection into a Supersonic Stream," M. S. thesis, Oct. 1969, U.S. Naval Postgraduate School, Monterey, Calif.

[4] Dahm, T. J., "The Development of an Analogy to Blast-Wave Theory for the Prediction of Interaction Forces Associated with Gaseous Secondary Injection into a Supersonic Stream," TN 9166-TN-3, May 1964, Vidya, Div. of Itek Corp., Palo Alto, Calif.

[5] Zukoski, E. E. and Spaid, F. W., "Secondary Injection of Gases into Supersonic Flow," *AIAA Journal*, Vol. 2, No. 10, Oct. 1964, pp. 1689–1696.